Paraelectric-Resonance Spectroscopy*

T. L. ESTLE
Physics Department, Rice University, Houston, Texas 77001
(Received 22 May 1968)

A theoretical description of paraelectric resonance is presented and analyzed in sufficient detail for comparison with experimental data on KCl. Some possible models for a paraelectric entity in relatively pure KCl are obtained, all of which can be distinguished from each other by further measurements. The simplest description and the one that fits best is a system of eight ⟨111⟩ dipoles with tunneling energy Δ_e of 10 GHz (a 21-GHz zero-field splitting) and an uncorrected electric-dipole moment μ of 7 D. This is consistent with substitutional Li^+ ions, but not with OH^- ions, which are known to be six ⟨100⟩ dipoles. Other less prominent structure was not explained by this description.

I. INTRODUCTION

PARAELECTRIC resonance is the electric analog of paramagnetic resonance. Electric dipole transitions are stimulated between states of a paraelectric imperfection in a crystalline solid by an oscillating electric field. Paraelectric imperfections occur in two or more differently oriented nuclear configurations in the crystal. The different configurations correspond to different orientations of the electric dipole moment of the imperfections and have the same energy in zero field. Paraelectric imperfections change their orientation by tunneling through the potential-energy barrier separating the various orientations. The most commonly studied paraelectric imperfections have been molecular impurities in alkali halides. The analogy between paraelectric resonance and paramagnetic resonance is poor in at least one important respect. Both the classical and the quantum-mechanical descriptions of paramagnetic resonance require the coupling of the magnetic dipole moment to the angular momentum. The electric dipole moment is not coupled to the angular momentum, if any, of the imperfection. The gyromagnetic coupling for paramagnetic entities results in energy levels and matrix elements of the time-varying Hamiltonian between some states of the system, and hence to resonance. For paraelectric resonance tunneling leads to both of these characteristics while the Stark effect for the discrete orientations of the dipoles also leads to discrete energies.

Paraelectric resonance is a new form of spectroscopy which should, in principle, possess a richness in its characteristics similar to that for other forms of spectroscopy. In addition, because of its basis in the vibrational and rotational characteristics of imperfections, it should provide information on systems with anharmonic vibrations and the closely related problem of hindered rotations. Because the imperfections are paraelectric and also paraelastic it is possible to obtain information on the electric and elastic interactions including the dynamic ones leading to relaxation. These features make the study of paraelectric resonance of fairly wide interest.

The importance of this subject has motivated many investigators to examine it experimentally or theoretically. The theoretical papers have usually concentrated on individual aspects of the subject. Thus many aspects of the theory have not been considered and a comprehensive discussion has not appeared. Similarly the experimental work to date has amply demonstrated the phenomenon and many of its features. However, no work has appeared giving sufficient detail either experimentally or theoretically to allow the theoretical interpretation of the experimental data to lead to a specific model or description of the paraelectric entity. That is to say the spectroscopic data has not led to an identification of the nature of the system studied.

The objects of this paper are to present a theoretical description of paraelectric resonance and to indicate what is required to compare theory with experiment. Several new or modified aspects of the theory will be discussed. The basic ideas in the theory will be illustrated using a bistable-dipole model. More realistic models for cubic crystals will then be discussed and compared to the experimental data reported for KCl. The models which can fit the data will be discussed. All theoretically calculated characteristics were obtained by diagonalizing the Hamiltonian, using the resultant eigenvalues and eigenfunctions to calculate relative transition rates.

II. SUMMARY OF THE DEVELOPMENT OF PARAELECTRIC RESONANCE

The subject of the paraelectricity and paraelasticity of imperfections in crystals, of which paraelectric resonance is a part, is relatively new but already very extensive. However, a very brief summary of some of the more important contributions should add perspective to the present paper.

The experimental development originated in two areas. One of these was the observation in alkali halides of the strong absorption of phonons observed in thermal conductivity by Klein[1] and Pohl[2] and observed in

* This work was supported by U. S. Air Force Office of Scientific Research Contract No. AF 49(638)-1250 at Texas Instruments Inc., and by National Aeronautic and Space Administration Grant No. NsG-6-59 at Rice University. The majority of the work was performed while the author was at the Physics Research Laboratory, Texas Instruments Inc., Dallas, Tex.

[1] M. V. Klein, Phys. Rev. **122**, 1393 (1961).
[2] R. O. Pohl, Phys. Rev. Letters **8**, 481 (1962).

acoustic attenuation by Brugger and Mason.[3] The other was the detailed study of the O_2^- molecule-ion impurity in potassium halides by Känzig.[4] Känzig used electron paramagnetic resonance to study the effects of applied static uniaxial stress on the energies of O_2^- ions and also to study the paraelastic relaxation times. Somewhat later Kuhn and Lüty[5] demonstrated the paraelectricity of OH^- ions in KCl by studying the dichroism of the uv optical absorption at low temperatures in high applied electric fields while Känzig, Hart, and Roberts[6] studied the dielectric constant of the same system and confirmed its paraelectricity in this way. At about the same time Narayanamurti[7] reported the infrared absorption of the CN^- ion in KCl and KBr below room temperature. These measurements verified a description of the CN^- in terms of hindered rotation. The demonstration that paraelectrics could be employed to perform adiabatic depolarization experiments in analogy with adiabatic demagnetization was made in KCl:OH^- by several authors[6,8] and for KCl containing Li^+ and CN^- by Lombardo and Pohl.[9] Further measurements of the dielectric constant of KCl:OH^- were made.[10] The dielectric constant of CN^-, NO_2^-, and Li^+ in several alkali halides was measured by Sack, and Moriarty.[11]

Since almost all characteristics of paramagnetism were demonstrated to have analogs in paraelectricity it was natural to look for paraelectric resonance as well. This led to successful observations in several laboratories at about the same time. It appears that a broad-line resonance spectrum was responsible for the microwave properties of KCl reported by Feher and Shepherd.[12] Bron and Dreyfus[13] reported a paraelectric resonance in KCl presumably associated with OH^- impurities. They worked at 9 GHz where their resolution was poor. Feher, Shepherd, and Shore[14] obtained better resolution by working at 35 GHz and, assuming OH^- dipoles responsible, obtained values for the tunneling energy and electric dipole moment that fit their data. Lakatos and Sack[15] studied the zero-field variant of paraelectric resonance in KCl:Li^+ and KCl:CN^-. Schearer and Estle[16,17] reported observations which also were assumed to arise from OH^- ions in KCl. From the microwave saturation of the resonance lines for three directions they found inconsistencies with a simple KCl:OH^- model. More recently Höcherl, Blumenstock, and Wolf[18] have obtained evidence suggesting that some of the paraelectric-resonance measurements on KCl have not been on the OH^- ion. Bron and Dreyfus[19] have recently published a more complete study of the paraelectric resonance of KCl than contained in their first letter.[13] However, their conclusions remain essentially the same. A very similar phenomenon has also been reported recently in smoky quartz by Kerssen and Volger.[20]

Theoretically the early work of Pauling[21] and especially Devonshire[22] led to an understanding of many of the gross features of the rotation of molecules hindered by the potential in a crystalline host.[23] Devonshire calculated the energy levels of a rigid linear molecule with fixed center of mass in an octahedral potential having the simplest possible mathematical form. His results have recently been refined by Sauer.[24] The importance of tunneling or inversion[25] was recognized by Bersuker, who analyzed a rather different problem.[26] He treated the Jahn-Teller effect[27] for Cu^{++} in octahedral or nearly octahedral coordination. This may be regarded as a paraelastic imperfection with nonzero electronic spin. Most of the remainder of the theory followed and was motivated by the experimental development previously described. Känzig's demonstration[4] that the O_2^- ions could reorient even at 1°K and his measured reorientation times led Sussmann to attempt an explanation involving tunneling.[28] His inability to explain the detailed measurements was subsequently shown by Pirc, Žekš, and Gosar[29] to result from an incorrect evaluation of the required matrix

[3] K. Brugger and W. P. Mason, Phys. Rev. Letters **7**, 270 (1961).
[4] W. Känzig, J. Phys. Chem. Solids **23**, 479 (1962).
[5] U. Kuhn and F. Lüty, Solid State Commun. **2**, 281 (1964).
[6] W. Känzig, H. R. Hart, Jr., and S. Roberts, Phys. Rev. Letters **13**, 543 (1964).
[7] V. Narayanamurti, Phys. Rev. Letters **13**, 693 (1964).
[8] U. Kuhn and F. Lüty, Solid State Commun. **3**, 31 (1965); I. Shepherd and G. Feher, Phys. Rev. Letters **15**, 194 (1965); I. W. Shepherd, J. Phys. Chem. Solids **28**, 2027 (1967).
[9] G. Lombardo and R. O. Pohl, Phys. Rev. Letters **15**, 291 (1965).
[10] U. Bosshard, R. W. Dreyfus, and W. Känzig, Phys. Condensed Matter **4**, 254 (1965).
[11] H. S. Sack and M. C. Moriarty, Solid State Commun. **3**, 93 (1965).
[12] G. Feher and I. Shepherd, Bull. Am. Phys. Soc. **10**, 735 (1965).
[13] W. E. Bron and R. W. Dreyfus, Phys. Rev. Letters **16**, 165 (1966).
[14] G. Feher, I. W. Shepherd, and H. B. Shore, Phys. Rev. Letters **16**, 500 (1966).
[15] A. Lakatos and H. S. Sack, Solid State Commun. **4**, 315 (1966).
[16] L. D. Schearer and T. L. Estle, Solid State Commun. **4**, 639 (1966).
[17] L. D. Schearer and T. L. Estle, in *Proceedings of the Fourteenth Colloque Ampère Ljubljana* (North-Holland Publishing Co., Amsterdam, 1967), p. 644.
[18] G. Höcherl, D. Blumenstock, and H. C. Wolf, Phys. Letters **24A**, 511 (1967).
[19] W. E. Bron and R. W. Dreyfus, Phys. Rev. **163**, 304 (1967).
[20] J. Kerssen and J. Volger, Phys. Letters **24A**, 647 (1967).
[21] L. Pauling, Phys. Rev. **36**, 430 (1930).
[22] A. F. Devonshire, Proc. Roy. Soc. (London) **A153**, 601 (1936).
[23] See N. L. Owen [Sci. Progr. **55**, 453 (1967)] for a recent review of the hindered rotation of free molecules.
[24] P. Sauer, Z. Physik **194**, 360 (1966); K. L. Jüngst and P. Sauer, *ibid.* **200**, 249 (1967).
[25] The term inversion is used by analogy with ammonia.
[26] I. B. Bersuker, Zh. Eksperim. i Teor. Fiz. **43**, 1315 (1962) [English transl.: Soviet Phys.—JETP **16**, 933 (1963)]; I. B. Bersuker and B. G. Vekhter, Fiz. Tverd. Tela **5**, 2432 (1963); **7**, 1231 (1965) [English transls.: Soviet Phys.—Solid State **5**, 1772 (1964); **7**, 986 (1965)]; Phys. Status Solidi **16**, 63 (1966).
[27] See, for example, C. J. Ballhausen, *Introduction to Ligand Field Theory* (McGraw-Hill Book Co., New York, 1962), pp. 193–208; and M. D. Sturge, in *Solid State Physics*, edited by F. Seitz, D. Turnbull, and H. Ehrenreich (Academic Press Inc., New York, 1967), Vol. 20, p. 91.
[28] J. A. Sussmann, Phys. Condensed Matter **2**, 146 (1964).
[29] R. Pirc, B. Žekš, and P. Gosar, J. Phys. Chem. Solids **27**, 1219 (1966).

elements rather than any fundamental misconception. The observation of paraelectric properties for Li impurities in alkali halides[9,11] led to attempts to explain the failure of the Li^+ ion to occupy the central and most symmetric place[30] and subsequently to a description of the lowest set of states which arise from tunneling.[31,32] The observation[6] of a concentration-dependent peak in the low-frequency dielectric constant as a function of temperature for OH^- in KCl led to many papers which attempted to explain these results. Most of these were concerned with the interactions between dipoles at high concentrations of OH^- and hence with the statistical mechanical features.[33] However, the work of Baur and Salzman[34] attempted to understand some of these observations using the concept of tunneling and the resultant properties of the lowest-lying states.

A detailed description of paraelectrics did not evolve until descriptions of paraelectric resonance appeared.[35–38] Then the values of the energy were obtained not only for no applied field but also for applied electric fields and stresses. In addition the effect of tunneling in coupling states and therefore in producing transitions was made evident. More recently a number of pertinent theoretical papers have appeared. These include the discussion by Vredevoe[39] of the relaxation time of OH^- dipoles in KCl and papers on several aspects of tunneling.[40,41] There has also been very great recent activity in nonresonance experimental studies, but since this paper is concerned primarily with paraelectric resonance, these will not be mentioned unless they are particularly pertinent to a later section.

III. THEORETICAL DESCRIPTION

Paraelectric imperfections in crystals have equivalent minima of their potential energy in zero field for more than one nuclear configuration. These different configurations correspond to different orientations of the electric dipole moment. Tunneling through the potential barriers[42] separating the minima will result in a mixing of the zero-point vibrational wave functions corresponding to each minimum and in energy splittings similar to the inversion splittings of the ammonia molecule. The mixing will lead to allowed electric dipole transitions between some of the states split by the tunneling. The mixing also allows transitions stimulated by interactions with the phonon strain and hence leads to relaxation. Application of an electric field produces further contributions to the energies and changes in the tunneling. Usually the electric field reduces the intensity of the transitions. In paraelectric resonance such electric dipole transitions are obtained by tuning the proper energy difference to resonance with the microwave quanta by means of an external uniform electric field.

The tunneling approximation[14,31,32,34–38] will be used in the majority of cases analyzed in this paper. In the tunneling approximation the barrier is high enough so that approximate solutions of the problem are the solutions of the harmonic-oscillator problems for each potential minimum. Thus the several displaced zero-point vibrational states are obtained. Separately, these are poor approximations of the true eigenstates (they do not have O_h symmetry) but because of tunneling for penetrable barriers one should take linear combinations in a manner analogous to the use of linear combinations of atomic orbitals as molecular orbitals in molecular quantum mechanics. Using the individual zero-point vibrational states as our basis states we find both overlap integrals and off-diagonal matrix elements of the Hamiltonian. We will consider only the limiting form of the tunneling approximation in which the overlap is neglected with respect to the effects of the off-diagonal matrix elements of the Hamiltonian (an approximation which is demonstrably valid at least in simple situations).

Even within the tunneling approximation one could attempt calculations from first principles in which all quantities such as tunneling energies and electric dipole moments are calculated. However, this is very difficult to do, particularly if one does not have a detailed knowledge of the nature of the paraelectric imperfection. In addition it considerably detracts from the elegance of calculations of the properties of paraelectric systems in terms of these quantities. Thus the various quantities characterizing the defect will be introduced into the theory as adjustable parameters. If the correct theory can be found describing a given set of experimental data, the magnitudes of these parameters can then be determined. This approach is analogous to that commonly used when employing a spin Hamiltonian in paramagnetic resonance.

[30] J. A. D. Matthew, Solid State Commun. **3**, 365 (1965); G. J. Dienes, R. D. Hatcher, R. Smoluchowski, and W. Wilson, Phys. Rev. Letters **16**, 25 (1966); W. D. Wilson, R. D. Hatcher, G. J. Dienes, and R. Smoluchowski, Phys. Rev. **161**, 888 (1967); R. J. Quigley and T. P. Das, Solid State Commun. **5**, 487 (1967); Phys. Rev. **164**, 1185 (1967).

[31] S. P. Bowen, M. Gomez, J. A. Krumhansl, and J. A. D. Matthew, Phys. Rev. Letters **16**, 1105 (1966).

[32] M. Gomez, S P. Bowen, and J. A. Krumhansl, Phys. Rev. **153**, 1009 (1967).

[33] W. Zernik, Phys. Rev. **139**, A1010 (1965); **158**, 562 (1967); R. Brout, Phys. Rev. Letters **14**, 175 (1965); M. W. Klein, Phys. Rev. **141**, 489 (1966); W. N. Lawless, Phys. Rev. Letters **17**, 1048 (1966); Phys. Condensed Matter **5**, 100 (1966).

[34] M. E. Baur and W. R. Salzman, Phys. Rev. Letters **16**, 701 (1966); Phys. Rev. **151**, 710 (1966).

[35] P. Sauer, O. Schirmer, and J. Schneider, Phys. Status Solidi **16**, 79 (1966).

[36] H. B. Shore, Phys. Rev. **151**, 570 (1966).

[37] G. Pfister, Helv. Phys. Acta **39**, 602 (1966).

[38] T. L. Estle, in *Proceedings of the Fourteenth Colloque Ampère, Ljubljana* (North-Holland Publishing Co., Amsterdam, 1967), p. 631.

[39] L. A. Vredevoe, Phys. Rev. **153**, 312 (1967).

[40] H. B. Shore, Phys. Rev. Letters **17**, 1142 (1966); J. A. Sussman, J. Phys. Chem. Solids **28**, 1643 (1967); W. N. Lawless, *ibid.* **28**, 1755 (1967); M. E. Baur and W. R. Salzman, Phys. Rev. Letters **18**, 590 (1967).

[41] C. Y. Fong, Phys. Rev. **165**, 462 (1968).

[42] We are here assuming the validity of the Born-Oppenheimer approximation for important nuclear configurations.

The actual form of the result depends on the point symmetry of the site occupied by the imperfection and by the point symmetry of the minimum-energy configurations. These two symmetries determine the number of equivalent minima. A general treatment would be very abstract and difficult to relate to experiment. Thus, for descriptive purposes, we will examine the simplest problem possessing all essential characteristics. This is the bistable dipole model having two equivalent potential minima.

A. Bistable Dipole Model

As an explicit form of the bistable dipole model consider C_s symmetry with the two dipoles canted with respect to the mirror plane[43] (see Fig. 1). If ψ_1 and ψ_2 are the zero-point vibrational wave functions corresponding to the two potential minima, then the only important matrix elements of the Hamiltonian are $\mathcal{H}_{12}=\mathcal{H}_{21}$, since the diagonal elements are equal to the zero-point energy which can be suppressed in our choice of the zero of energy. Since $\mathcal{H}_{12}$ is normally negative,[44] we will write it as $-\Delta$, where Δ is greater than zero and is the first parameter introduced. Application of external electric fields or stresses will result in a linear coupling to the imperfections for which the constants of proportionality are, respectively, $\mathfrak{y}$, the electric dipole moment (vector), and $\mathfrak{\lambda}$, the elastic dipole moment (tensor).[45] These can be considered classically or in a somewhat more elegant and simpler fashion they can be taken as operators whose diagonal matrix elements have the classical values. Although there will be several components in general for $\mathfrak{y}$ and $\mathfrak{\lambda}$, those components leading to equal displacements of the zero-point energy of the two basis states can be suppressed by the choice of the zero of energy. Thus only components splitting the previously degenerate zero-point energies need be explicitly included. This is the z component of $\mathfrak{y}$ and the xz component of $\mathfrak{\lambda}$ (where the x axis is chosen to eliminate the yz component of $\mathfrak{\lambda}$).

The full Hamiltonian matrix becomes

$$\mathcal{H}_{ij}=\begin{pmatrix}-\mu\mathcal{E}_z-\lambda T_{xz} & -\Delta \\ -\Delta & \mu\mathcal{E}_z+\lambda T_{xz}\end{pmatrix},$$

where Δ, μ, and λ are parameters, $\mathcal{E}_z$ is the z component of the applied electric field, and T_{xz} is the xz component of the applied stress. The solution of this eigenvalue problem or its generalizations together with the use of this same Hamiltonian to describe stimulated transitions from applied high-frequency electric or elastic fields and also to describe relaxation leads to all of the features of paraelectrics and paraelastics, including resonance, and will be the basis for all of the results presented in this paper.

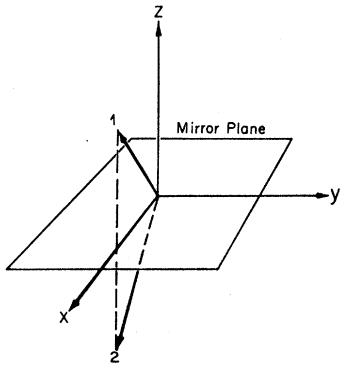

FIG. 1. The dipoles, coordinate axes, and mirror plane for the bistable dipole model with C_s symmetry. The z component of the electric field and the xz component of the shear stress act differently on the two orientations of the dipole.

Neglecting overlap, as we will do throughout, and for simplicity considering the applied stress to be zero, we obtain the energy eigenvalues

$$E_\pm=\pm[(\mu\mathcal{E}_z)^2+\Delta^2]^{1/2},$$

which are plotted in Fig. 2.

The zero-field eigenfunctions are $\psi_\pm=(1/\sqrt{2})(\psi_2\mp\psi_1)$. The state corresponding to the symmetric function, ψ_- has energy $-\Delta$ and the antisymmetric state has the

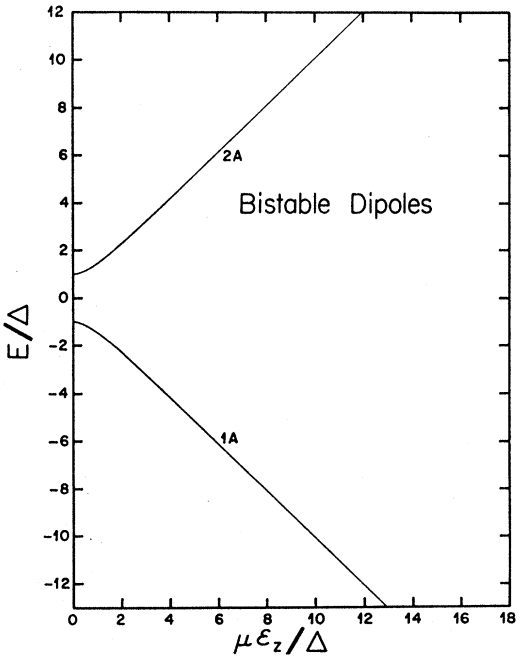

FIG. 2. The energy levels as a function of the z component of the electric field for the bistable dipole model.

[43] This choice is made in order to have different elastic properties for the two and thus to lead naturally to elastic dipole relaxation.

[44] To obtain this result it is necessary to use both the kinetic and potential energy rather than just the potential energy as done in the second paper of Ref. 34.

[45] A. S. Nowick and W. R. Heller, Advan. Phys. **12**, 251 (1963); **14**, 101 (1965). We are using the applied rather than the local or internal fields and our $\mathfrak{y}$ and $\mathfrak{\lambda}$ reflect this. Note that our $\mathfrak{\lambda}$ differs from the Nowick and Heller definition by the molecular volume.

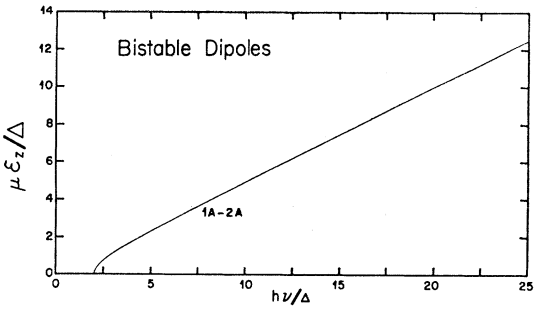

FIG. 3. The value of the z component of the electric field at which resonance occurs as a function of the frequency of the oscillating electric field along the z axis for the bistable dipole model.

energy Δ. These results are the same as those in the description of the NH_3 inversion spectrum.

At high field ψ_- becomes ψ_1 and ψ_+ becomes ψ_2 and the energies are just minus and plus $\mu\mathcal{E}_z$. If an oscillating electric field is applied parallel to z then an electric dipole transition is allowed by symmetry and occurs when

$$h\nu = 2[(\mu\mathcal{E}_z)^2+\Delta^2]^{1/2},$$

where ν is the frequency of the oscillating electric field. The static electric field at which the resonance occurs is shown as a function of the frequency in Fig. 3, where the threshold frequency arising from the zero-field energy difference is clearly evident. The intensity of the transition calculated from rather awkward expressions for the wave functions is proportional to I,

$$I \equiv |\langle\psi_+|\mu_z\mathcal{E}_{1z}|\psi_-\rangle|^2 = \mu^2\mathcal{E}_{1z}^2\frac{\Delta^2}{(\mu\mathcal{E}_z)^2+\Delta^2} = \mu^2\mathcal{E}_{1z}^2\frac{4\Delta^2}{(h\nu)^2},$$

where $\mathcal{E}_{1z}$ is the amplitude of the oscillating electric field. Since only relative measurements will be used, the only part of the expression for the intensity that we need is I. The intensity goes down rapidly with frequency above the threshold as is shown in Fig. 4. The effects of externally applied stress and random static internal elastic and electric fields can be readily examined with this model. The random internal fields lead to a breadth in the observed resonance line (inhomogeneous broadening).[41,46]

Relaxation can occur in many ways. Because of the strong coupling to applied fields it is reasonable to assume rapid relaxation by coupling to the strain (stress) of phonons. At low temperatures this would involve transitions between pairs of states that are coupled by elastic dipole matrix elements and would be accompanied by the absorption or emission of one phonon.[47] At higher temperatures multiphonon processes become important,[48] as does the process in which electric dipole coupling occurs. The latter results because of the electric field produced by the gradient of the phonon strain. By expressing the phonon strain in terms of creation and annihilation operators, relating this to the stress via the elastic constants, and inserting this into the expression for the one-phonon thermal transition rate one generally obtains[49]

$$W_{ij} = \frac{(\hbar\omega)^3}{\exp(\hbar\omega/kT)-1}\sum_{a,b,m,n} R_{abmn}\langle i|\lambda_{ab}|j\rangle\langle i|\lambda_{mn}|j\rangle, \quad (1)$$

where W_{ij} is the one-phonon stimulated elastic dipole transition rate from state i to state j, ω is the phonon frequency ($\hbar\omega$ is the energy difference between the states), and the fourth-rank tensor R_{abmn} depends only on parameters for the crystal and not on the imperfection, the temperature, or the phonon energy. In the high-temperature limit ($\hbar\omega \ll kT$) there is an explicit dependence of W_{ij} upon ω^2 arising from the quadratic energy dependence of the density of states of phonons at low energies. For the bistable dipole in the high-temperature limit, Eq. (1) becomes

$$W_{+-} = 16kTR_{xzxz}\lambda^2\Delta^2,$$

i.e., the result is independent of electric field or energy difference since the matrix elements of λ are proportional to $1/\omega$ (as shown by the similarity of λ and μ and the expression for I). Thus we find, in contrast to the electric dipole transitions stimulated by the oscillating electric field, that the relaxation rate is not quenched at high fields or frequencies. It has, of course, the proportionality to temperature required of a direct process at high temperatures.

Considerations similar to those leading to Eq. (1) and involving the interaction of the electric dipole moment with the phonon's electric field give

$$W_{ij} = \frac{(\hbar\omega)^5}{\exp(\hbar\omega/kT)-1}\sum_{a,b} Q_{ab}\langle i|\mu_a|j\rangle\langle i|\mu_b|j\rangle$$

for the one-phonon stimulated electric dipole relaxation rate, where Q_{ab} again depends only on crystal parameters. Particularizing to the bistable dipole case we obtain

$$W_{+-} = 4kTQ_{zz}\mu^2\Delta^2\hbar^2\omega^2 = 16kTQ_{zz}\mu^2\Delta^2[(\mu\mathcal{E}_z)^2+\Delta^2].$$

All of the calculations of relaxation and transition rates have assumed that the Hamiltonian describing the static behavior is the same as the one required at microwave frequencies.

[46] A. M. Stoneham, Rev. Mod. Phys. (to be published).

[47] What is called elastic dipole relaxation in this paper would appear to be what is called the noncentrosymmetric process by Vredevoe in Ref. 39. It is the same mechanism postulated by Sussman (Ref. 28) to explain the reorientation times of O_2^- in KCl and developed in a perturbation scheme by Pirc, Žekš, and Gosar (Ref. 29).

[48] This in fact continues until thermionic emission results at high temperatures [see J. A. Sussman, J. Phys. Chem. Solids **28**, 1643 (1967)].

[49] The analogous magnetic calculation is discussed in P. L. Donoho, Phys. Rev. **133**, A1080 (1964); K. W. H. Stevens, Rept. Progr. Phys. **30**, 189 (1967).

Paraelectric resonance experiments yield measurements of the position and intensity of resonance lines. They may also give information about the relaxation times. Schearer and Estle[16] investigated this by observing the microwave power saturation of the paraelectric resonance transitions in KCl. Saturation occurs whenever the transition rate caused by the applied oscillating field exceeds the transition rate resulting from relaxation. The intensity of the power absorption is proportional to $P(1+SP)^{-1}$ when the individual homogeneously-broadened lines are lifetime broadened where S is proportional to I/W_{+-}^2 for the bistable dipole case. More generally the relaxation rate in the denominator of S is the total rate between the two levels including all processes with one or more real intermediate states. In the bistable dipole case we obtain

$$S \propto (\mu^2/\lambda^4\Delta^2\omega^2T^2). \quad (2)$$

One could also assume that the homogeneous width is not governed by the lifetime. This would lead to a somewhat different expression than Eq. (2) for S, presumably proportional to T^{-1}. Experimental data[16] cannot distinguish between the two at present although the temperature dependence appears to be near the values of T^{-1} and T^{-2} expected.

The bistable dipole model can be used to analyze many other features of paraelectric and paraelastic imperfections. These include interactions, effects of applied uniaxial stresses, paraelastic resonance, and the statistical response of the system as described by a density matrix. The density matrix description leads to the coexistence of resonance and relaxation for the bistable dipole model and by induction also in all paraelectric systems in which investigations are made with oscillating and static fields parallel. Such a behavior is quite different from that usually encountered in paramagnetic systems. The bistable dipole model can also be used to analyze more general descriptions than allowed by the tunneling approximation. One such approach is taken up in the next section.

B. Symmetry-Limited Description

A somewhat more general approach is to determine the zero-field symmetry characteristics of the lower states (those to be described), and then to write down the most general Hamiltonian matrix involving these states which is allowed by symmetry and linear in electric fields and stresses. This would usually consist of using the states expected for tunneling to indicate the symmetry but not the actual form of the lower states. The effect of this is to produce a more complex coupling to fields than in the simple tunneling approach employed earlier. This process is similar to the generalized spin Hamiltonian introduced in electron paramagnetic resonance.[50] For the bistable dipole problem of the previous section we now have a ten-parameter description instead of a four-parameter one using Δ, μ, λ, and the orientation of the axes in the xy plane. The matrix of the Hamiltonian in terms of the A' and A'' states (the zero-field eigenstates corresponding to symmetric and antisymmetric combinations, respectively) is

$$\mathcal{H}_{ij}=\begin{bmatrix} -\Delta-\mu_x\mathcal{E}_x-\mu_y\mathcal{E}_y-\lambda_{xy}T_{xy} & & -\mu_z\mathcal{E}_z-\lambda_{xz}T_{xz}-\lambda_{yz}T_{yz} \\ & -\lambda_{xx}T_{xx}-\lambda_{yy}T_{yy}-\lambda_{zz}T_{zz} & \\ -\mu_z\mathcal{E}_z-\lambda_{xz}T_{xz}-\lambda_{yz}T_{yz} & & \Delta+\mu_x\mathcal{E}_x+\mu_y\mathcal{E}_y+\lambda_{xy}T_{xy} \\ & +\lambda_{xx}T_{xx}+\lambda_{yy}T_{yy}+\lambda_{zz}T_{zz} & \end{bmatrix}.$$

Similar, but more complex, expressions can be obtained for the models discussed in later sections.

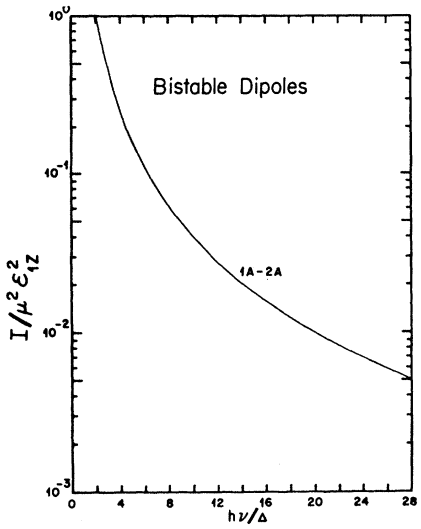

FIG. 4. The relative intensity versus the frequency for the bistable dipole model with the oscillating electric field parallel to the static field.

C. Six ⟨100⟩ Dipoles

This and all remaining sections will deal with crystals having octahedral point symmetry (O_h). This corresponds to the symmetry of the alkali halides in which the vast majority of all work on paraelectricity has been done. In order to interpret experimental data we need to know the properties expected of all types of dipoles which can occur in O_h symmetry. This task is simplified by the fact that as the dipole gets lower in symmetry and therefore more complex, the expected results get more complex. Hence, if the observed results are simple we may truncate our search procedure and examine only the simpler cases. For the simplest case the dipoles have C_{4v} symmetry, i.e., the dipoles are oriented along the six possible ⟨100⟩ crystalline axes. This case has been examined by several authors.[14,32,35–38]

[50] See A. Bieri and F. K. Kneubühl, Phys. Condensed Matter **4**, 230 (1965), and references cited therein.

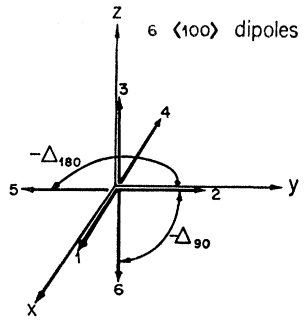

FIG. 5. The six dipoles, the cubic axes, and the two types of tunneling for the six-⟨100⟩-dipole model.

With no applied electric field or stress the wave functions are the linear combinations of the six zero-point vibrational functions, ψ_i, which transform into themselves under the symmetry operations of the cube (this is similar to symmetric and antisymmetric for the bistable dipole case). The dipole directions are labelled in Fig. 5 which also shows the two types of neighbors (90° and 180°) which produce the two types of $\mathcal{H}_{ij}$ from tunneling. These wave functions are (using the tunneling approximation and neglecting overlap as usual)

$$\psi_{A_{1g}}=(1/\sqrt{6})(\psi_1+\psi_2+\psi_3+\psi_4+\psi_5+\psi_6),$$
$$\psi_{E_g}=\tfrac{1}{2}(\psi_1+\psi_4-\psi_2-\psi_5);\quad (1/2\sqrt{3})(2\psi_3+2\psi_6-\psi_1-\psi_2-\psi_4-\psi_5),$$
$$\psi_{T_{1u}}=(1/\sqrt{2})(\psi_1-\psi_4);\ (1/\sqrt{2})(\psi_2-\psi_5);\ (1/\sqrt{2})(\psi_3-\psi_6).$$

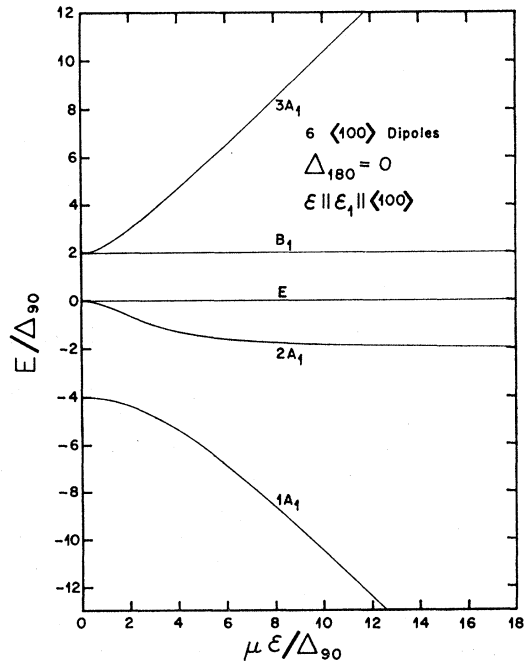

FIG. 6. The energy levels versus the electric field for the six-⟨100⟩-dipole model, $\Delta_{180}=0$, and the electric field applied along a ⟨100⟩ axis.

The energies of these three states are readily seen to be

$$E_{A_{1g}}=-4\Delta_{90}-\Delta_{180},$$
$$E_{T_{1u}}=\Delta_{180},$$
$$E_{E_g}=2\Delta_{90}-\Delta_{180}.$$

All really simple descriptions of tunneling either for rotating diatomic molecules or for displaced small ions suggest that the tunneling involving the least geometrical change (the smallest change in the nuclear configuration) should dominate, presumably 90° tunneling in this case. However, it may be dangerous to rely on generalizing this simple argument particularly when it was noticed that such a theory would not fit experiment for what was thought to be a verified case of six ⟨100⟩ dipoles.[16] Hence the six-⟨100⟩-dipole model has been investigated for a variety of values of Δ_{180}/Δ_{90} including all qualitatively different possibilities.[51]

Because of the symmetry the interaction with an electric field and a stress can be described in terms of one parameter each within the tunneling approximation. Excluding stress the full Hamiltonian matrix is

$$\mathcal{H}_{ij}=\begin{pmatrix} -\mu\mathcal{E}_x & -\Delta_{90} & -\Delta_{90} & -\Delta_{180} & -\Delta_{90} & -\Delta_{90} \\ -\Delta_{90} & -\mu\mathcal{E}_y & -\Delta_{90} & -\Delta_{90} & -\Delta_{180} & -\Delta_{90} \\ -\Delta_{90} & -\Delta_{90} & -\mu\mathcal{E}_z & -\Delta_{90} & -\Delta_{90} & -\Delta_{180} \\ -\Delta_{180} & -\Delta_{90} & -\Delta_{90} & \mu\mathcal{E}_x & -\Delta_{90} & -\Delta_{90} \\ -\Delta_{90} & -\Delta_{180} & -\Delta_{90} & -\Delta_{90} & \mu\mathcal{E}_y & -\Delta_{90} \\ -\Delta_{90} & -\Delta_{90} & -\Delta_{180} & -\Delta_{90} & -\Delta_{90} & \mu\mathcal{E}_z \end{pmatrix}. \tag{3}$$

The major consequences arise from introducing various components of $\mathcal{E}$, solving for the energies and eigenfunctions and using the eigenfunctions to calculate intensities, relaxation rates, and saturation parameters. For simple orientations of $\mathcal{E}$ symmetry allows the reduction of the matrix and one occasionally finds solutions of the eigenvalue problem that are simple analytic expressions. More generally, numerical calculations are required.

For the electric field parallel to ⟨100⟩ the symmetry is reduced from O_h to C_{4v} and three types of states occur (labelled A_1, B_1, and E). An example of the electric field dependence of the energy levels[52] is shown in Fig. 6 for $\Delta_{180}=0$. Of more value in analyzing paraelectric resonance data is the position of the lines in field at various frequencies, shown in Fig. 7 for two values of Δ_{180}/Δ_{90}. The transitions shown are those allowed by symmetry

[51] Independent of Δ_{180}/Δ_{90} there are selection rules at zero applied field which influence the subsequent results for applied fields. These are that only odd (u) to even (g), i.e., A_{1g} to T_{1u} and E_g to T_{1u}, paraelectric resonance transitions are allowed and only even (g) to even (g), A_{1g} to E_g, relaxation via the direct elastic dipole mechanism is allowed. The evenness of the elastic dipole operator arises because it is the coupling constant between energy and stress.

[52] Sauer, Schirmer, and Schneider (Ref. 35), Shore (Ref. 36), and Gomez, Bowen, and Krumhansl (Ref. 32) show plots of E versus $\mathcal{E}$ for $\mathcal{E}$ parallel to ⟨100⟩, ⟨111⟩, and ⟨110⟩ directions. Pfister (Ref. 37) also discusses such plots for $\mathcal{E}$ along the ⟨100⟩ and ⟨111⟩ directions.

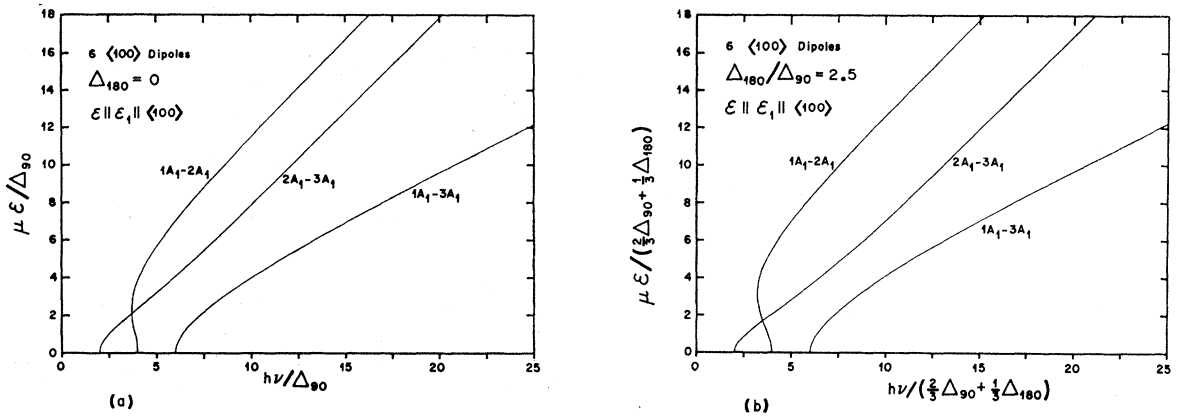

FIG. 7. The electric fields at resonance versus the frequency of the oscillating electric field for the six-⟨100⟩-dipole model, both fields along ⟨100⟩, and (a) $\Delta_{180}=0$, (b) $\Delta_{180}/\Delta_{90}=2.5$.

when the oscillating and static electric fields are parallel as they have been in all experiments to date. Additional helpful information should result from other geometrical arrangements as well. The relative intensities of these transitions are plotted in Fig. 8 against frequency using the same two values of Δ_{180}/Δ_{90}. Plots similar to those in Fig. 7 and 8 were published earlier by this author.[38]

In the present case the expression for the direct elastic dipole relaxation rate given in Eq. (1) reduces to

$$W_{ij}=\frac{(\hbar\omega)^3}{\exp(\hbar\omega/kT)-1}(R_{zzzz}-R_{xxyy})\times(\langle i|\lambda_{xx}|j\rangle^2+\langle i|\lambda_{yy}|j\rangle^2+\langle i|\lambda_{zz}|j\rangle^2).$$

The relative elastic dipole relaxation rates in the high-temperature limit are plotted as a function of field in Fig. 9 for $\Delta_{180}=0$. The total relaxation rate between any pair of A_1 levels comes into the expressions for saturation and these are shown in Fig. 10 for $\Delta_{180}=0$ and elastic dipole coupling.[53] The main conclusion to be obtained from these and many other calculations for other values of Δ_{180}/Δ_{90} is that the relaxation rates appearing in the saturation parameter are all approximately the same and almost independent of frequency. Exceptions occur near zero field (i.e., near the threshold frequencies) where zero-field selection rules influence the results. We therefore conclude that the observed saturation behavior gives a measure of the relative intensities (electric dipole transition rates) under most experimental conditions.

The eigenvalue problem for the matrix in Eq. (3) is greatly simplified by choosing simple directions of the field and is quite different for the various simple directions. Thus a comparison of the results for the electric

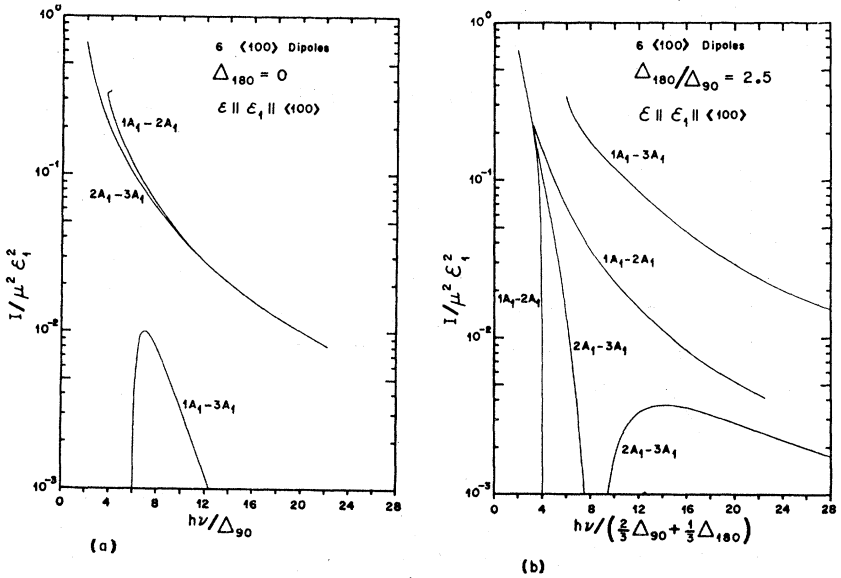

FIG. 8. The relative intensities of the paraelectric resonance transitions as a function of the frequency of the oscillating electric field for the six-⟨100⟩-dipole model, both fields along ⟨100⟩, and (a) $\Delta_{180}=0$, (b) $\Delta_{180}/\Delta_{90}=2.5$.

[53] The total relaxation rate includes all combinations of one or more direct processes that join the two levels in question. The process is similar to that of calculating the conductance of a complicated circuit.

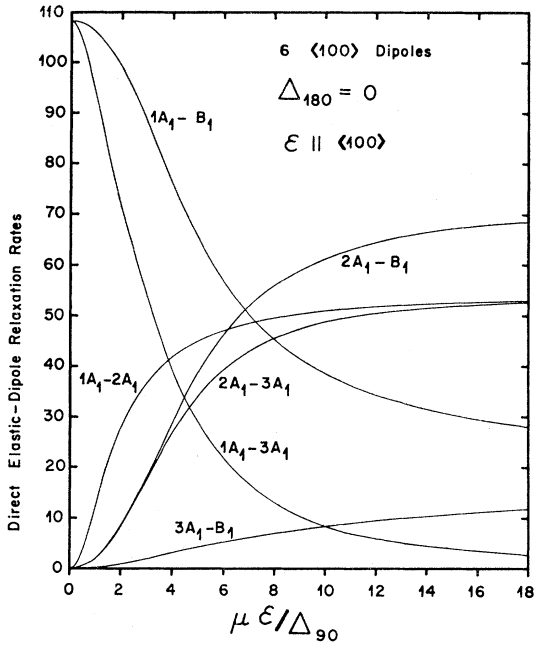

FIG. 9. Direct elastic dipole-relaxation rates versus electric field for six ⟨100⟩ dipoles, $\Delta_{180}=0$, and for the electric field in a ⟨100⟩ direction. The high-temperature limit is assumed and the rates are only relative.

field along ⟨100⟩, ⟨111⟩, and ⟨110⟩ directions is quite useful. For the electric fields along a ⟨111⟩ direction the energy levels are plotted by Sauer, Schirmer, and Schneider.[35] The position of the resonance line in field for various frequencies is shown in Fig. 11 for $\Delta_{180}=0$ and $\Delta_{180}/\Delta_{90}=2.5$. The most significant result is probably the failure of a line to appear with a threshold frequency of $6\Delta_{90}/h$ for the case, $\Delta_{180}=0$. The intensities of these transitions are shown in Fig. 12 and the total elastic dipole relaxation rate is shown in Fig. 13 for $\Delta_{180}=0$. Again the saturation factor will depend primarily on the intensity except near zero field. Also

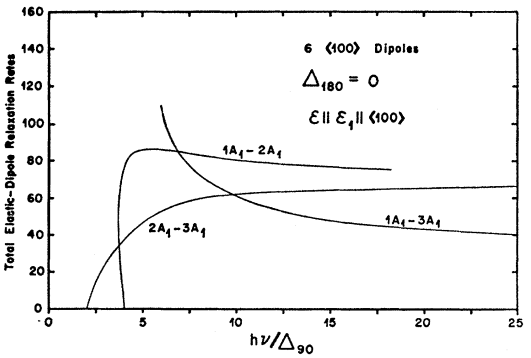

FIG. 10. Total elastic dipole-relaxation rates versus electric field for six ⟨100⟩ dipoles, $\Delta_{180}=0$, and both electric fields along a ⟨100⟩ direction. The total rates consist of all possible combinations of direct rates which join the two levels being saturated. The high-temperature limit is assumed and the rates are only relative.

the total relaxation rates are about the same[54] as the values shown in Fig. 10 for the fields along ⟨100⟩.

The results for the electric fields parallel to a ⟨110⟩ direction are qualitatively similar in many important respects to those for ⟨100⟩. The nature of these results is illustrated by a plot of the positions and intensities of the transitions for $\Delta_{180}=0$ in Figs. 14 and 15. As before the total relaxation rates are nearly constant and about equal to those for fields along ⟨100⟩.

The predictions for other directions of the electric field, for simultaneous stress, and for a transverse oscillating electric field have interesting characteristics which may be useful in comparisons with experiment. The present experimental results do not justify the presentation of these calculations.

In Sec. IIIB we discussed the more general approach in which the Hamiltonian is determined primarily by restrictions imposed by symmetry. In the present case of an A_{1g}, and E_g, and a T_{1u} state we need two parameters (such as Δ_{90} and Δ_{180}) to describe the tunneling and two parameters (instead of one μ) to specify the Stark effect. The effect of stress requires still more parameters since a tensor is the coupling constant (the number is six for this case).

D. Eight ⟨111⟩ Dipoles

The next simplest case occurring for O_h symmetry is eight dipoles along the ⟨111⟩ axes each dipole having C_{3v} symmetry. The properties of this system have been discussed by Gomez, Bowen, and Krumhansl.[32] They show plots of the variation of energy with electric field assuming cube edge tunneling[55] and for $\mathcal{E}$ along ⟨100⟩, ⟨111⟩, and ⟨110⟩ axes. For the case $\Delta_f=\Delta_b=0$ which is physically the most reasonable of the simple possibilities and for the electric fields along a ⟨100⟩, ⟨110⟩, or ⟨111⟩ axis, the positions of the allowed transitions are shown in Fig. 16 and the intensities for the fields along ⟨100⟩ are shown in Fig. 17. Only one resonance line will be observed experimentally at a given orientation since all allowed transitions are coincident. In addition these superimposed transitions all have a threshold frequency of $2\Delta_e/h$, the lowest possible value. The intensities and relaxation rates are approximately independent of the orientation of the fields among these three directions. Thus the results for eight ⟨111⟩ dipoles are simple.

E. Twelve ⟨110⟩ Dipoles

After six ⟨100⟩ dipoles and eight ⟨111⟩ dipoles the next simplest case is twelve ⟨110⟩ dipoles. As will be

[54] For a fixed value of Δ_{180}/Δ_{90}, the calculated results for intensities and relaxation rates are normalized the same so that comparisons can be made for different angles.

[55] There are now three parameters describing the tunneling, Δ_e for tunneling between dipoles along a cube edge from each other, Δ_f for those across a face, and Δ_b for those through the body diagonal. The parameter Δ_e would usually correspond to tunneling between the closest nuclear configurations.

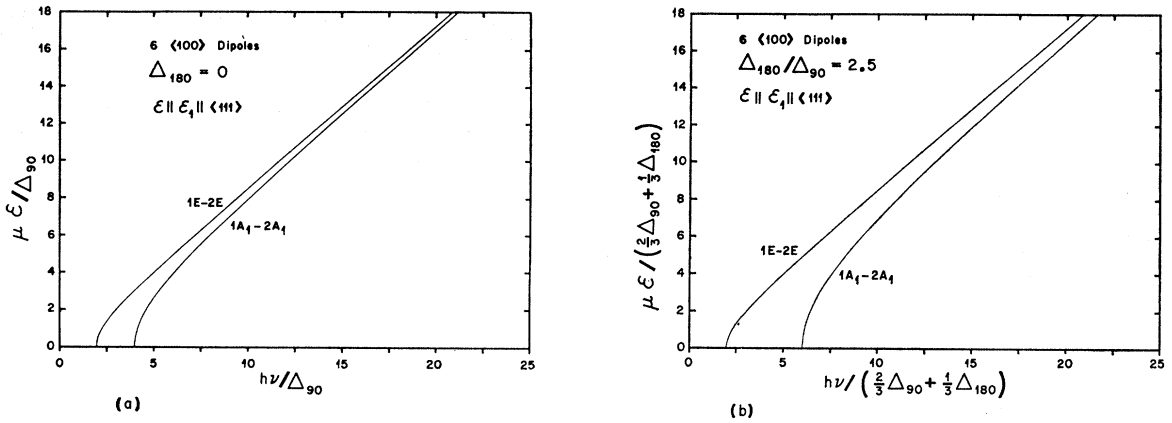

FIG. 11. The electric fields at resonance versus the frequency of the oscillating electric field for the six-⟨100⟩-dipole model, both fields along ⟨111⟩, and (a) $\Delta_{180}=0$, (b) $\Delta_{180}/\Delta_{90}=2.5$.

indicated these results are already considerably more complex than the two already discussed. Any model more complex than this can be assumed to yield results of still greater complexity. Thus, at present it does not appear necessary to consider these models (higher-frequency measurements should definitely confirm or contradict this assertion). For twelve ⟨110⟩ dipoles there are four energy parameters describing tunneling. Again we will neglect all but the one parameter corresponding to tunneling between the nuclear configurations which are closest. For this case we can see some of the complexity by examining Figs. 18–20 in which the energy level diagram, the position of the resonances in electric field, and their intensities are plotted for the electric fields parallel to ⟨100⟩.

There has been some speculation[56] about the possibility that OH^- in KCl is really more complex than six ⟨100⟩ dipoles but that an A_{1g}, a T_{1u}, and an E_g state are lower than all others and the only states thermally populated at a few degrees Kelvin.[57] This behavior may occur and is somewhat more difficult to verify or discriminate against. However, it should be possible to analyze such a system using a symmetry-restricted Hamiltonian. Thus if it deviates in behavior from six ⟨100⟩ dipoles it should do so in a way which can be fairly easily analyzed.

IV. COMPARISON WITH EXPERIMENTS

Despite the numerous paraelectric resonance experiments which have been performed there is insufficient

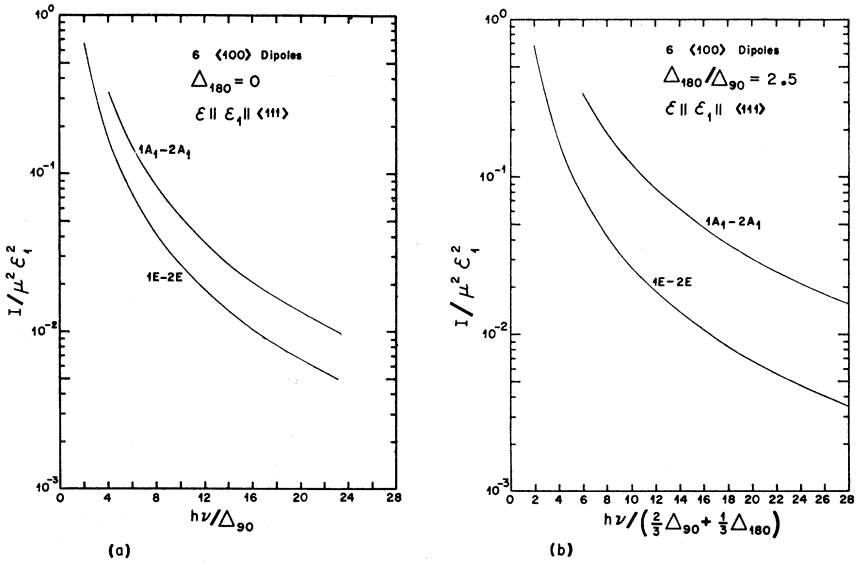

FIG. 12. The relative intensities of the paraelectric resonance transitions as a function of the frequency of the oscillating electric field for the six-⟨100⟩-dipole model, both fields along ⟨111⟩, and (a) $\Delta_{180}=0$, (b) $\Delta_{180}/\Delta_{90}=2.5$.

[56] O. Schirmer and J. Schneider (private communication); last paper of Ref. 40.

[57] For 24 dipoles in either the {100} or {110} planes with tunneling among the four dipoles nearest each ⟨100⟩ direction greatest, one can consider the symmetric combination of these four dipoles for each of the six ⟨100⟩ directions as approximating one of the lowest states. These each act like a single ⟨100⟩ dipole and from weaker tunneling they combine to give A_{1g}, E_g, and T_{1u} states just like for six ⟨100⟩ dipoles. There would of course be 18 other states at higher energies.

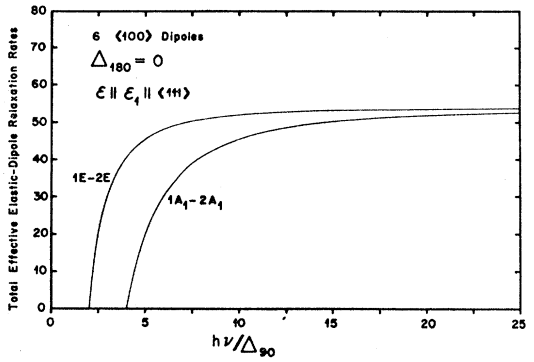

FIG. 13. Total elastic dipole relaxation rates versus electric field for six ⟨100⟩ dipoles, $\Delta_{180}=0$, and both electric fields along a ⟨111⟩ direction. The high-temperature limit is assumed and the rates are only relative.

data reported on any system to allow meaningful comparison with theory except for KCl.[58] The major results in undoped or OH^--doped KCl are summarized below[14,16] (all experiments are done with static and microwave electric fields parallel and with the crystal at temperatures near 1°K):

(i) At a frequency of about 24.6 GHz the spectra[16] for electric fields parallel to ⟨100⟩, ⟨111⟩, and ⟨110⟩ are

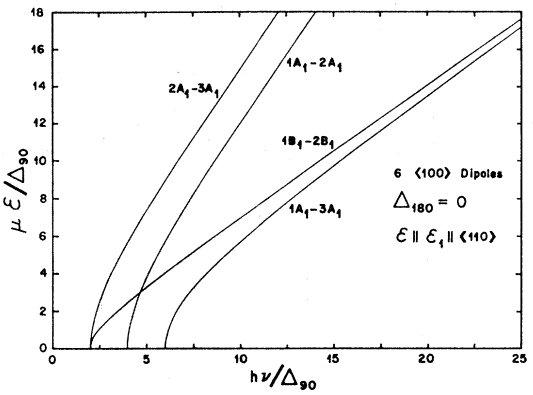

FIG. 14. The electric fields at resonance versus the frequency of the oscillating electric field for the six-⟨100⟩-dipole model, both fields along ⟨110⟩, and $\Delta_{180}=0$.

each dominated by one line whose peak-to-peak intensity in derivative display considerably exceeds any other structure that may be present. These three lines are comparable in intensity, are all broad with a width comparable to their position in field, and with positions near 3–5 kV/cm. The ordering in field is $\mathcal{E}_{100}<\mathcal{E}_{110}<\mathcal{E}_{111}$ with the fields differing by less than a factor of 2.

(ii) At 28.8 GHz[59] and 35.2 GHz[14] less information is available but the existing results are consistent with the description given in (i), with the lines at higher field for a higher frequency.

(iii) The lines corresponding to the three orientations in (i) saturate at very nearly the same power.[60]

(iv) Other structure is seen at higher field[14,16] for 24.6 and 35.1 GHz, especially for $\mathcal{E}$ along ⟨100⟩.

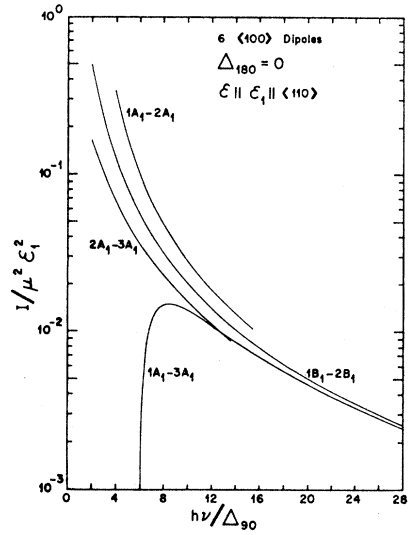

FIG. 15. The relative intensities of the paraelectric resonance transitions as a function of the frequency of the oscillating electric field for the six-⟨100⟩-dipole model, both fields along ⟨110⟩, and $\Delta_{180}=0$.

(v) Poorly resolved lines are seen[13,14,19] at frequencies near 9 GHz with the shape of both the absorption and the dispersion depending on the orientation.[61] The intensities appear roughly comparable to those at higher frequencies.

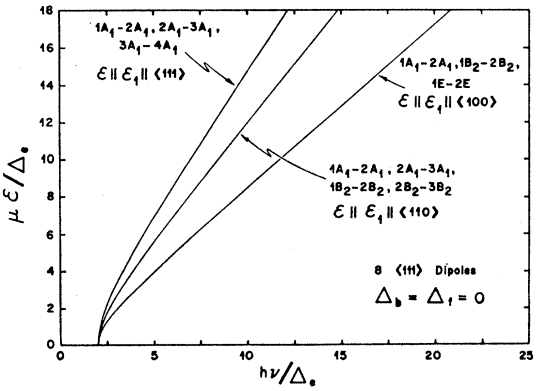

FIG. 16. The electric fields at resonance versus the frequency of the oscillating electric field for the eight-⟨111⟩-dipole model, both fields along ⟨111⟩, ⟨110⟩, or ⟨100⟩, and $\Delta_b=\Delta_f=0$.

[58] The data of Dreyfus [Bull. Am. Phys. Soc. 12, 351 (1967)] on RbCl:CN^- may also be adequate but is not yet available in published form.

[59] J. Carnes and R. Timme (private communication).

[60] Subsequent measurements [L. D. Schearer (private communication)] indicate more scatter than shown in Ref. 16. However, the saturation factors are still equal to better than a factor of 5.

[61] Recently better resolution has been reported at 9 GHz [R. W. Dreyfus, Bull. Am. Phys. Soc. 13, 500 (1968)].

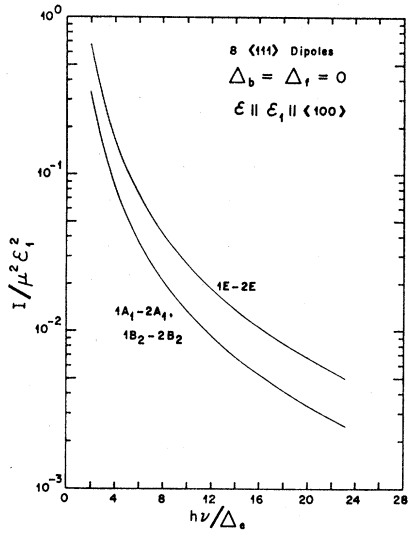

FIG. 17. The relative intensities of the paraelectric resonance transitions as a function of the frequency of the oscillating electric field for the eight-⟨111⟩-dipole model, both fields along ⟨100⟩, and $\Delta_b = \Delta_f = 0$.

The most reliable and most abundant data seem to arise from the prominent low-field lines at high frequency (24.6 GHz or above). Thus in seeking an explanation let us start by comparing the various theoretical models to these data. The reproducibility of these lines and their similarities upon varying several experi-

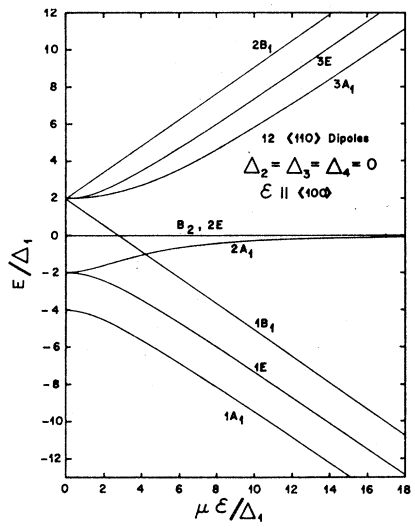

FIG. 18. The energy levels versus the electric field for the twelve-⟨110⟩-dipole model, nearest configuration tunneling ($\Delta_2 = \Delta_3 = \Delta_4 = 0$), and the electric field applied along a ⟨100⟩ axis.

mental parameters suggests that they are all from the same imperfection. Since other structure is sometimes observed, let us assume at first that everything arises from one paraelectric imperfection. Since these spectra have been observed in the purest available KCl, let us also assume that the imperfections are isolated. Finally, let us assume that the inhomogeneous broadening mechanisms will not shift the peak or change the apparent intensities or relaxation times so that we can compare to the predicted results for a perfect environment. This point can be checked theoretically and the inhomogeneous broadening does appear to have a rather small effect, at least in some cases.

Our assumptions lead us to examine the possible models for the high measuring frequencies above the

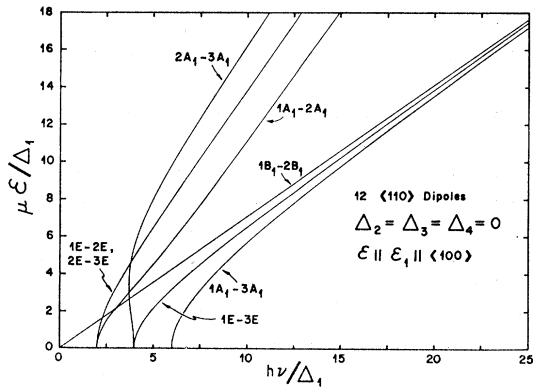

FIG. 19. The electric fields at resonance versus the frequency of the oscillating electric field for the twelve-⟨110⟩-dipole model, both fields along ⟨100⟩, and $\Delta_2 = \Delta_3 = \Delta_4 = 0$.

second threshold frequency in order to explain the high-field structure. The frequency dependence of the position of the prominent observed lines suggests that this threshold would occur around 21 GHz so that the data taken at 24.6 GHz can be regarded as taken just above threshold. Let us first examine the model usually suggested,[13,14,19,36,37] that of six ⟨100⟩ dipoles and $\Delta_{180} = 0$. If we are above the highest-frequency threshold

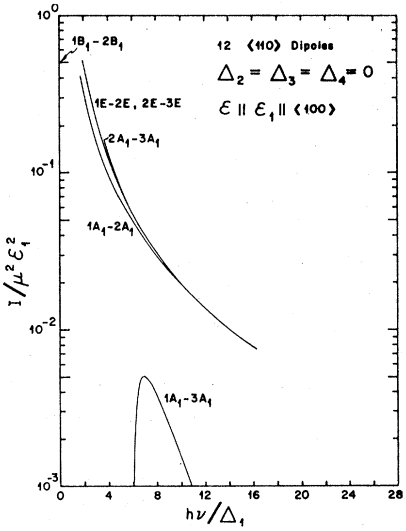

FIG. 20. The relative intensities of the paraelectric resonance transitions as a function of the frequency of the oscillating electric field for the twelve-⟨110⟩-dipole model, both fields along ⟨100⟩, and $\Delta_2 = \Delta_3 = \Delta_4 = 0$.

then the low-field lines for the three directions, ⟨100⟩, ⟨111⟩, and ⟨110⟩ are in the order $\mathcal{E}_{100}<\mathcal{E}_{110}<\mathcal{E}_{111}$ but $\mathcal{E}_{111}$ is roughly 50% too high in field to fit the data [compare Figs. 7(a), 11(a), and 14 at $h\nu/\Delta_{90}=7$]. The intensities of the prominent lines for these three orientations differ by an order of magnitude leading to almost a two order of magnitude difference in the saturation parameter when the relaxation rates are included.[62] This is in clear contrast with observation.[16,60] In addition the intensities, positions, and saturation behavior of the higher-field structure does not fit this model. Thus this model does not describe the observations well.

Nothing qualitatively important occurs for nonzero Δ_{180} until it becomes comparable with Δ_{90}. The most striking effects occur when it is larger than Δ_{90} and such that the outermost states in zero field have opposite parity (T_{1u} and A_{1g} or T_{1u} and E_g). Since the zero-field selection rules influence the behavior at low frequencies the results are now quite different and we find that all of the observations listed above can be explained by these models (using for example $\Delta_{180}/\Delta_{90}=2.5$ or -3.5) if we are above the highest-frequency threshold.

It might also be possible to fit the data using the six-⟨100⟩-dipole model if the experimental frequencies (except 9 GHz) are above the second threshold frequency. However, the order of the levels would be wrong for $\Delta_{180}=0$. In addition the experiments[14] at 35.2 GHz would then be above the highest threshold and would give different results than those obtained. Similar difficulties, although not quite so severe, attend explanations involving Δ_{180}/Δ_{90} near 2.5, -3.5, and many other values.

If we try to use one model, i.e., one imperfection, to explain all of the results then for six ⟨100⟩ dipoles it seems necessary to assume a very large 180° tunneling. Another possibility that merits serious consideration is that two or more imperfections may be contributing to the results listed above. The recent work of Höcherl, Blumenstock, and Wolf[18] together with the correlation of paraelectric resonance to the presence of OH^- in KCl suggests this possibility. If this is so we would be better off explaining only the prominent low-field high-frequency lines. The results are still the same for the six-⟨100⟩-dipole model except that we must now consider also the possibility of being just above the lowest-frequency threshold. This explanation would appear to fit for $\Delta_{180}/\Delta_{90}=0$, 2.5, and -3.5 as well as many other values. This possibility can most effectively be checked for many values of Δ_{180}/Δ_{90} including zero by looking for other structure at frequencies above 42 GHz.

Let us next consider the eight-⟨111⟩-dipole model with only cube-edge tunneling. This of course fails to reproduce all of the data but gives exactly and very simply the observations on the prominent lowest-field high-frequency lines. No unusual assumptions as to the tunneling are required. For fields parallel to ⟨100⟩, ⟨111⟩, and ⟨110⟩ this model would yield no other lines at higher frequency and will differ qualitatively from any of the six-⟨100⟩-dipole models when the effects of varying frequency, stress, and orientation are fully exploited.

Finally the twelve-⟨110⟩-dipole model and any more complex possibility is too complex to fit the observed data no matter whether all or part of the structure is thought to arise from the imperfection and independent of which of the threshold frequencies is correlated to the 21-GHz experimental value.

Thus, we see that there are three reasonable descriptions of the experimental data. These are

(i) Six ⟨100⟩ dipoles with Δ_{180}/Δ_{90} of about 2.5 or -3.5 and with the measuring frequencies above 24 GHz exceeding the high-frequency threshold. This would explain qualitatively and semiquantitatively all of the high-frequency structure as well as the 9-GHz results. It suffers from the disadvantages of requiring a tunneling which may not appear physically plausible and of not agreeing quite as well with theory as it should. This last point is not very definite since the broad, sometimes asymmetric, lines are hard to measure with sufficient accuracy. The parameters[63] obtained for $\Delta_{180}/\Delta_{90}=2.5$ are $\Delta_{90}/h=2.3$ GHz, $\Delta_{180}/h=5.8$ GHz, and $\mu=4.0$ D.

(ii) Eight ⟨111⟩ dipoles with nearest configuration tunneling. This explains all of the properties of the prominent high-frequency lines very well, but requires a second unspecified imperfection to explain the other structure and the 9-GHz results. The parameters obtained are discussed below.

(iii) Six ⟨100⟩ dipoles with 24.6 GHz just above the lowest-frequency threshold. The fit is usually not quite as good as for description (ii) depending on Δ_{180}/Δ_{90} but probably within experimental error. The parameters obtained for $\Delta_{180}=0$ are $\Delta_{90}/h=10.5$ GHz and $\mu=5.0$ D.

The three possibilities can be unambiguously distinguished if sufficient data are obtained for various frequencies, orientations, applied stresses, and other experimental parameters. On the basis of present evidence it appears that the eight-⟨111⟩-dipole model is to be favored as the explanation. This is the behavior ascribed to Li^+ ions when substituting for K^+ in KCl. This suggests the possibility that it may be Li^+ or some other small positive ion such as H^+ (remember the

[62] The high-temperature functional forms of the relaxation rates in our theoretical development are independent of T and thus easy to plot and analyze. However, at temperatures near 1°K there are corrections of the order of a factor of 2 that need to be applied to our calculated rates. This is most significant in comparing low-field and high-field lines. For six ⟨100⟩ dipoles this is important only when used to try to explain all observed lines. In this case it strengthens the argument that the $\Delta_{180}=0$ case cannot fit the observed data.

[63] All values of μ are uncorrected for the difference between the local internal field and the external field.

experiments of Höcherl, Blumenstock, and Wolf[18]). If the eight-⟨111⟩-dipole model is adjusted to have the proper scale to fit the experimental results then the tunneling energy Δ_e is 10 GHz and the splitting between adjacent levels in zero field is 21 GHz (0.7 cm^{-1} or 0.5°K) and the total over-all splitting is 63 GHz (2.1 cm^{-1} or 1.5°K). The uncorrected electric dipole moment obtained is 7 D. This may suggest an appreciable off-center location as for Li^+ or possibly H^+. The known Li^+ results are similar in magnitude for the zero-field splitting[11] but do not give quite as large an electric dipole moment.[9,64] However, H^+ would probably displace more than Li^+ and might lead to a value this large.[65]

Since the data on KCl analyzed in this paper are best explained in terms of eight ⟨111⟩ dipoles, the implication is that OH^- impurities are not the responsible imperfections. The OH^- impurities in KCl were shown to be six ⟨100⟩ dipoles by Kuhn and Lüty[5] and Härtel and Lüty.[66] However, OH^- may contribute to some of the less prominent structure that the present analysis did not explain.

It may be objected that more consideration should be given to the departures from a simple system. These include the effects of the inhomogeneous broadening mechanisms on the apparent position, intensity, and saturation behavior of the lines; the possibilities of other relaxation mechanisms[67]; interactions; and field inhomogeneities. Calculations on these effects suggest that they are not of major importance. Sufficient redundancy in the comparisons of experiment and theory should eliminate any such possibilities.

V. CONCLUSIONS

Although of recent origin, the phenomenon of paraelectric resonance has a firm foundation both experimentally and theoretically. We have analyzed a number of models using in part existing theoretical ideas together with some new concepts and formulations. Some of the results of this analysis are presented and compared to the existing data on KCl. An insufficient variety of experimental data has been obtained to unambiguously distinguish between several potential models. To more fully exploit the spectroscopic potential of paraelectric resonance it will be necessary to make observations chosen so as to distinguish the various possible models. They differ enough in detail that by varying the orientation of $\mathcal{E}$ and independently of $\mathcal{E}_1$, by varying frequency, by simultaneous application of stress, by paraelastic resonance, by the study of absorption and dispersion, and by studying the microwave saturation it should be possible to find a unique model that fits the data. Only then will paraelectric resonance demonstrate its potential value for solid-state physics.

ACKNOWLEDGMENTS

The author wishes to acknowledge the contributions of numerous colleagues with whom various aspects of this work have been discussed. In particular it is a pleasure to acknowledge the early stimulating discussions and correspondence with J. Schneider and the long collaboration with L. D. Schearer. The generous assistance of Charles Ratliff in writing the program used for these calculations is acknowledged. The comments of G. K. Walters, B. Dischler, J. Carnes, and R. Timme on the manuscript were useful. The opportunity to work on this subject provided by Texas Instruments Incorporated is gratefully acknowledged.

[64] The uncorrected electric dipole moment of Ref. 9 is 5.51 D for any of the models considered in the present paper. However, the accuracy of their measurement or ours may be worse than stated and these two values may be the same.

[65] Recent measurements by Höcherl and Wolf give strong evidence that it is indeed Li^+ [G. Höcherl and H. C. Wolf, Phys. Letters **27A**, 133 (1968)].

[66] H. Härtel and F. Lüty, Phys. Status Solidi **12**, 347 (1965).

[67] We have not considered the possible role that a phonon bottleneck might play. Cross relaxation may occur; hence a possibility exists that another fast relaxing species is responsible for the observed relaxation.